

See discussions, stats, and author profiles for this publication at: <https://www.researchgate.net/publication/8387624>

Self-assembling of Helical Poly(Phenylacetylene) Carrying l -Valine Pendants in Solution, on Mica Substrate, and on Water Surface

ARTICLE *in* LANGMUIR · SEPTEMBER 2004

Impact Factor: 4.46 · DOI: 10.1021/la036118l · Source: PubMed

CITATIONS

35

READS

15

7 AUTHORS, INCLUDING:



Shi-Zhao Kang

Shanghai Institute of Technology

114 PUBLICATIONS 926 CITATIONS

SEE PROFILE



Lian-Sheng Ling

Sun Yat-Sen University

45 PUBLICATIONS 801 CITATIONS

SEE PROFILE



Ben Zhong Tang

The Hong Kong University of Science and Tec...

785 PUBLICATIONS 28,958 CITATIONS

SEE PROFILE

Self-assembling of Helical Poly(Phenylacetylene) Carrying L-Valine Pendants in Solution, on Mica Substrate, and on Water Surface

Bing Shi Li,^{†,‡} Shi Zhao Kang,[†] Kevin K. L. Cheuk,[‡] Lijun Wan,[†]
Liansheng Ling,[†] Chunli Bai,^{*,†} and Ben Zhong Tang^{*,‡}

Center for Molecular Sciences, Institute of Chemistry, Chinese Academy of Sciences, China;
and Department of Chemistry, Hong Kong University of Science & Technology,
Hong Kong, China

Received November 11, 2003. In Final Form: March 25, 2004

In the present work, we investigated self-assembling of a poly(phenylacetylene) carrying L-valine pendants (PPA-Val) in a water/methanol solution, upon evaporation of the solution on mica, and on the water surface. With intercalation of a fluorescence probe of Ru(phen)₂(dppx)²⁺ (phen = 1,10-phenanthroline, dppx = 7,8-dimethyldipyridophenazine) into the hydrophobic cavities associated by the PPA-Val chains, their helical structures were directly detected in solution with an in situ fluorescence microscope. Helical aggregates were observed with AFM upon evaporation of the solvents, suggesting that the helical structures in the solution are the building blocks of the helical aggregates. Self-assembling structures of PPA-Val on the water surface were, however, very different from that formed upon evaporation of its THF solution on the mica surface. The polymer chains associated into a monolayer of extended fibers on the water surface, whereas superhelical fibers formed on the mica surface. Water molecules play a critical role in inducing the polymer to form diverse morphological structures in its bulk solution and on its surface. In solution, the isotropic hydrophobic effect drove the polymer chains to form superhelical aggregates, while on the water surface, the hydrophobic effect concentrated mainly on the lateral part of the polymer, thus giving a monolayer of extended fibers.

Introduction

Helical assemblies of natural polymers have attracted considerable interest due to their critical role in life science.¹ By mimicking the ways used by natural polymers, such as hydrogen bonding and hydrophobic effect, helical architectures can also be constructed using synthetic chiral polymer building blocks.² Circular dichroism (CD) spectrum is the major method to confirm the existence of helicity of chiral polymers,³ but it cannot offer detailed information about the self-assembling behaviors of the chiral polymers. In contrast to the dominant role of optical spectrum analysis on the optical activities of helical polymers, exploration on the corresponding self-assembling morphologies remains in its infancy. In this regard, TEM, SEM, and AFM can make an important complementary role in revealing the self-assembled structures formed by chiral molecules under selective conditions.^{4–6}

Samples are ordinarily prepared by evaporating the solvents and they are suggested to reflect the native assemblies. AFM equipped with a fluid cell can satisfy both directness and visual detection in solution,⁷ but this approach has seldom been successfully used in detecting the self-assemblies formed by polymers due to the involved complexity and difficulty in stabilizing the sample on the substrate. Until now, new attempts to satisfy a direct detection of the self-assemblies of helical polymer in solution remained an intractable task.

Self-assembling behaviors of chiral molecules on the surface/interface also draw intensive attention,⁸ and have a number of potential applications. The morphology of the self-assembled structures of the monolayer on a water surface differs from that formed in solution, because the noncovalent interactions that govern the self-assembly of chiral molecules are obviously different under these two conditions. For example, the hydrophobic repulsions between polymer chains and water molecules are remarkably different on the surface of water and in the bulk solution. The chiral molecules will thus adopt different self-assembling manners to satisfy the balances between chiral molecules and the corresponding environments, giving to different self-assembling morphologies. As a result, a single molecule may demonstrate diverse optical and electrical properties due to the different self-associations of the molecules under different conditions.⁹ A good understanding of the formation of the hierarchical

* Corresponding authors. Phone: +86-10-82614350. Fax: +86-10-82614350. E-mail: clbai@iccas.ac.cn (C.B.); Phone: +852-2358-7375. Fax: +852-2358-1594. E-mail: tangbenz@ust.hk (B.Z.T.).

[†] Chinese Academy of Sciences.

[‡] Hong Kong University of Science & Technology.

(1) Lehninger, A. L.; Nelson, D. L.; Cox, M. M. *Principles of Biochemistry*, 2nd ed.; Worth Publishers: New York, 1993.

(2) (a) Green, M. M.; Park, J.; Sato, T.; Teramoto, A.; Lifson, S.; Selinger, R. L. S.; Selinger, J. *Angew. Chem., Int. Ed. Engl.* **1999**, *38*, 3138–3154. (b) Nelson, J. C.; Saven, J. G.; Moore, J. S.; Wolynes, P. G. *Science* **1997**, *277*, 1793–1796. (d) Alper, J. *Science* **2002**, *295*, 2396–2397. (e) Cuccia, L. A.; Lehn, J. M.; Homo, J. C.; Schmutz, M. *Angew. Chem., Int. Ed.* **2000**, *39*, 233–237. (f) Aoki, T.; Kobayashi, Y.; Kaneko, T.; Kaneko, T.; Oikawa, E.; Yamamura, Y.; Fujita, Y.; Teraguchi, M.; Nunura, R.; Musuda, T. *Macromolecules* **1999**, *32*, 79. (g) Shinohara, K.; Yasuda, S.; Kato, G.; Fujita, M.; Shigekawa, H. *J. Am. Chem. Soc.* **2001**, *123*, 3619–3620.

(3) *Circular Dichroism: Principles and Applications*, 2nd ed.; Berova, N.; Nakanishi, K.; Woody, R. W., Eds.; Wiley-VCH: New York, 2000. (4) Akagi, K.; Piao, G.; Kaneko, S.; Sakamaki, K.; Shirakawa, H.; Kyotani, M. *Science* **1998**, *282*, 1683–1686.

(5) Fuhrhop, J.; Helfrich, W. *Chem. Rev.* **1993**, *93*, 1565–1582.

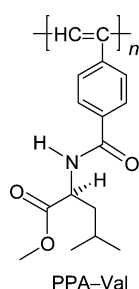
(6) Li, B. S.; Check, K. K. L.; Salhi, F.; Lam, J. W. Y.; Cha, J. A. K.; Xiao, X.; Bai, C.; Tang, B. Z. *Nano Lett.* **2001**, *1*, 323–328.

(7) Drake, B.; Prater, C. B.; Weisenhorn, A. L.; Gould, S. C.; Albecht, T. R.; Quate, C. F.; Cannell, D. S.; Hansma, H. G.; Hansma, P. K. *Science* **1989**, *243*, 1586.

(8) Zhang, Y. J.; Song, Y.; Zhao, Y.; Li, T. J.; Jiang, L.; Zhu, D. *Langmuir* **2001**, *17*, 1317–1320.

(9) Cheuk, K. K. L.; Lam, J. W. Y.; Chen, J.; Lai, L. M.; Tang, B. Z. *Macromolecules* **2003**, *36*, 5947–5959.

Chart 1



architectures thus becomes necessary prior to a successful use of the molecules with desired functions.

Herein, we report different self-assembling behaviors of chiral polymers under different environments. A series of chiral polyacetylenes carrying amino acids pendants was synthesized,¹⁰ and the simple chemical structures and novel self-assembling behaviors make these kinds of polymers ideal models to completely explore the relationship between the assemblies and corresponding conditions. The introduction of the fluorescence binding method not only provides an important new attempt to directly capture the self-assemblies in solution, it experimentally confirms the existence of the hydrophobic cavities in the hierarchical architectures. Thorough pictures of the self-assembling morphologies of PPA are presented: the assemblies made upon natural evaporation of solvent imaged with AFM, the assemblies recorded directly in solution with in situ fluorescence microscope, and the assemblies prepared with Langmuir–Blodgett film technique on the water surface. In addition, the comparisons between the diverse assemblies offer valuable information in helping to comprehensively characterize the factors related with the self-assemblies of chiral molecules under different conditions and optimizing their potential applications.

Experimental Section

AFM Measurements. A poly(phenylacetylene) containing L-valine moiety (PPA-Val; Chart 1) was synthesized using [Rh-(nbd)Cl]₂ as the catalyst according to the procedure described in our previous publication.¹¹ An AFM sample of the polymer was prepared by allowing a droplet (4 μ L) of a diluted polymer solution of desired concentration to evaporate on the surface of mica under ambient conditions. AFM measurements were performed on a Nano IIIa atomic force microscope (Digital Instruments, Santa Barbara, CA) operating in tapping mode using hard silicon cantilever tips with a spring constant of \sim 40 N/m.

Fluorescence Spectra and Images. Ru(phen)₂(dppx)²⁺(BF₄)₂·3H₂O (phen = 1,10-phenanthroline, dppx = 7,8-dimethyldipyridophenazine) was synthesized according to the previously reported method¹² and the crude product was recrystallized from ethanol three times and then characterized by ¹H NMR.¹² The stock solution of Ru(phen)₂(dppx)²⁺ was prepared by dissolving Ru(phen)₂(dppx)²⁺(BF₄)₂·3H₂O in ultrapure water obtained from a Millipore Milli-Q water purification system (resistivity = 18.2 M Ω cm) and further diluted with methanol/water (10:1 by volume) into a desired concentration (\sim 0.02 mM). Fluorescence spectra were measured in the diluted water/methanol solution on a Hitachi F-4500 spectrophotometer excited at 450 nm. Fluorescence images of PPA-Val were recorded with an *epi*-fluorescence microscope Axiovert 200 (Zeiss, Germany) equipped with AxioCam CCD (Zeiss, Germany). Coverslips were purchased from Fisher

Scientific Co. (Pittsburgh, United States). A droplet (\sim 20 μ L) of PPA-Val solution (\sim 0.386 mM) in the water/methanol mixture was sandwiched between two pieces of the coverslips.

Langmuir Film. The π -A isotherm of PPA-Val on the subphase of H₂O was measured at 23 \pm 1 $^{\circ}$ C, using a Sigma 70 Cam 200 LB 5000 trough (length 364 mm \times width 75 mm), equipped with a Wilhelmy platinum plate. Ultrapure water was used as the subphase. After ensuring that the water surface was clean, \sim 210 μ L of a THF solution of PPA-Val (330 μ g/mL) was spread on the water surface using a microsyringe. The π -A isotherms were measured after allowing the film to equilibrate for 15 min by closing the barriers at a constant rate of 10 mm/min. LB films of PPA-Val were transferred to a newly cleaved mica at 5 mm/min, at a surface pressure of 28 mN/m.

Results and Discussions

Self-assemblies of Helical Polymer in Solution and on Mica Substrate. In the design of the molecular structure of PPA-Val, we incorporated L-valine methyl ester into the polyacetylene structure with the hope that the bulky chiral pendants would exert an asymmetric force field on the polymer backbone to induce the macromolecular chain to adopt a helical conformation. As reported in our previous paper, the CD spectrum of PPA-Val showed intense absorption at 368 nm,¹¹ whereas its monomer showed no ellipticity, suggesting that a helical conformation has been taken by the backbone of the polymer. CD spectra, however, provide just general information of the existence of helicity formed by PPA-Val and we therefore try to reveal more details of the molecular self-assembling via other methods.

Ru(II) complexes have attracted great interest for their interactions with DNA obeying a “Light Switch” mechanism: they show no luminescence in aqueous solution, but emit remarkably high fluorescence in the presence of DNA by intercalating to the hydrophobic internality of DNA.¹³ By fluorescence binding with Ru(II) complexes, the morphologies of DNA can be recorded with an in situ fluorescence microscope and dynamic biochemical reactions are captured in solution. Since the self-assembling of the PPA-bearing amino acid attachments shares similarity with DNA in the molecular amphiphilicity and manners to construct helical structure, they may also possess hydrophobic cavities inside the helical structures in the polar solvent. Thus, it is natural to think that the fluorescence binding method might also be adopted in the exploration of the self-assembled structures formed by these kinds of helical polymers in solution.

Inspired by this idea, we first tested the possibility to employ the fluorescence binding method in the analysis of the self-assembled structures formed by this kind of PPA, bearing naturally appearing valine, leucine, and alanine, respectively. The fluorescence probe employed in the experiment is Ru(phen)₂(dppx)²⁺, which obeys a light-switch mechanism and is sensitive to the presence of a hydrophobic environment.¹⁴ A water/methanol mixture (V_{methanol}:V_{water} = 1:10) instead of pure methanol is used in the experiment in order to quench the fluorescence probe prior to the addition of polymer solution. Fluorescence spectrum measurement was performed in order to confirm the binding of Ru(phen)₂(dppx)²⁺ to the hydrophobic internality of the PPA-bearing amino acid attachments. This kind of PPA demonstrates similar trends in

(10) For reviews, see: (a) Tang, B. Z. *Polym. News* **2001**, 26, 262–272. (b) Tang, B. Z.; Cheuk, K. K. L.; Salhi, F.; Li, B. S.; Lam, J. W. Y.; Cha, J. A. K.; Xiao, X. *ACS Symp. Ser.* **2001**, 812, 133–148. (c) Cheuk, K. K. L.; Li, B. S.; Tang, B. Z. *Curr. Trends Polym. Sci.* **2002**, 7, 41–55.

(11) Li, B. S.; Cheuk, K. K. L.; Ling, L.; Chen, J.; Xiao, X.; Bai, C.; Tang, B. Z. *Macromolecules* **2003**, 36, 77–85.

(12) Amouyal, E.; Homs, A.; Chambron, J. C.; Sauvage, J. P. *J. Chem. Soc., Dalton Trans.* **1990**, 1841.

(13) Ling, L.; He, Z.; Song, G.; Zeng, Y. E.; Wang, C. Bai, C.; Chen, X.; Shen, P. *Anal. Chim. Acta* **2001**, 436, 207–214.

(14) (a) Hartshorn, R. M.; Barton, J. K. *J. Am. Chem. Soc.* **1992**, 114, 5919–5925. (b) Friedman, A. E.; Chambron, J. C.; Sauvage, J. P.; Turro, N. J.; Barton, J. K. *J. Am. Chem. Soc.* **1990**, 112, 4960–4962. (c) Monchern, C.; Kirsch-De, A.; Sylviachoua, M. *Inorg. Chem.* **1997**, 36, 584–592.

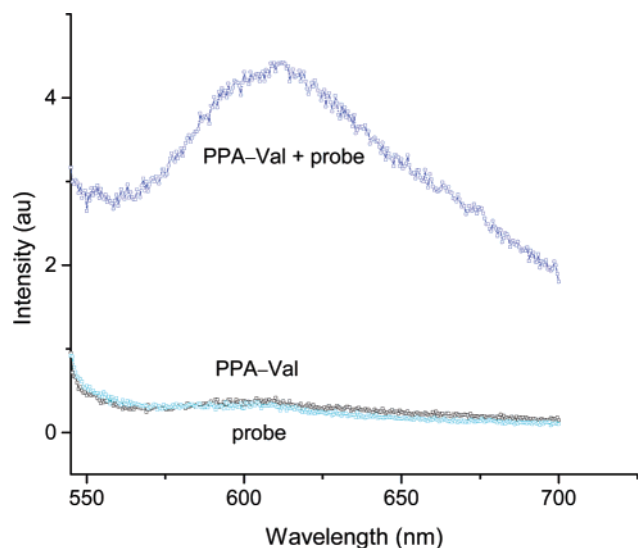


Figure 1. Fluorescence spectra of $\text{Ru}(\text{phen})_2(\text{dppx})^{2+}$, PPA-Val, and a mixture of PPA-Val and $\text{Ru}(\text{phen})_2(\text{dppx})^{2+}$ in water/methanol solution ($V_{\text{water}}:V_{\text{methanol}} = 10:1$) recorded on Hitachi F-4500 spectrophotometer. Excitation wavelength: 450 nm, concentration of PPA-Val: ~ 0.386 mM, and concentration of $\text{Ru}(\text{phen})_2(\text{dppx})^{2+}$: ~ 0.02 mM.

the fluorescence spectra with and without the addition of $\text{Ru}(\text{phen})_2(\text{dppx})^{2+}$ and only the spectra of PPA-Val is provided here (Figure 1). It is found that both PPA-Val and $\text{Ru}(\text{phen})_2(\text{dppx})^{2+}$ showed no emission at 610 nm. However, when $\text{Ru}(\text{phen})_2(\text{dppx})^{2+}$ was added to the polymer solution, a fluorescence spectrum peak at 610 nm was observed, which corresponds to the emission of $\text{Ru}(\text{phen})_2(\text{dppx})^{2+}$. The result is in full agreement with the interaction of $\text{Ru}(\text{phen})_2(\text{dppx})^{2+}$ with DNA,¹² indicating that $\text{Ru}(\text{phen})_2(\text{dppx})^{2+}$ has intercalated to the hydrophobic cavities of the helical polymer. PPA-Val is an amphiphilic polymer, consisting of hydrophobic and hydrophilic parts. In highly polar solvents, the polymer chains will self-assemble into structures with the hydrophobic part buried inside and the hydrophilic part exposed outside, leading to the formation of multiple hydrophobic pockets inside the helical structures. Those with suitable sizes will favor the intercalation of the fluorescence probes and electron transfer from the probes to water molecules can be effectively interrupted. The intercalation of the fluorescence molecules into the helical structures for the first time experimentally discloses the internal property of the helical structures in the polar solvent. The intercalation of the fluorescence probe to the hydrophobic cavities of the helical polymer also opens a new door to directly observe the self-assembled structures of PPA-Val in solution.

With in situ and real-time fluorescence imaging techniques, the helical structures formed by the polymer can be directly captured in solution with the intercalation of $\text{Ru}(\text{phen})_2(\text{dppx})^{2+}$ to the hydrophobic internality. As shown in Figure 2, in the absence of $\text{Ru}(\text{phen})_2(\text{dppx})^{2+}$, the polymer does not show a clear contour due to rather weak fluorescence emitted by the polymer itself. However, with an addition of $\text{Ru}(\text{phen})_2(\text{dppx})^{2+}$ to the solution, the green color of the superhelical aggregate is found to change to yellow, owing to the intercalation of $\text{Ru}(\text{phen})_2(\text{dppx})^{2+}$. More detailed characteristics of the helical trajectory of the polymer can thus be resolved, thanks to the strong light emitted by the fluorescence molecules. It can be seen clearly that the helical polymer demonstrates a left-handed twist (marked with arrows) prior to the formation of right-handed superhelical aggregates.

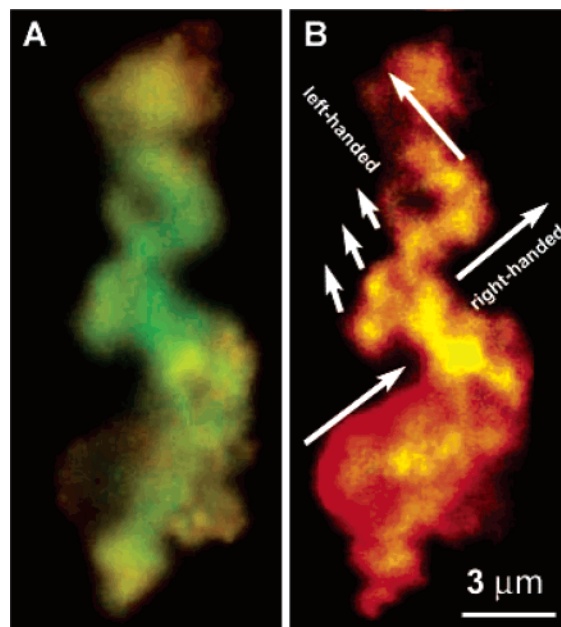


Figure 2. Fluorescence images of PPA-Val (A) without and (B) with an addition of $\text{Ru}(\text{phen})_2(\text{dppx})^{2+}$ ($V_{\text{water}}:V_{\text{methanol}} = 10:1$) imaged with *epi*-fluorescence microscope Axiovert 200 (Zeiss, Germany). Concentration of PPA-Val: ~ 0.386 mM, concentration of $\text{Ru}(\text{phen})_2(\text{dppx})^{2+}$: ~ 0.02 mM. The change of the polymer emission from green to yellow indicates that $\text{Ru}(\text{phen})_2(\text{dppx})^{2+}$ has intercalated to the polymer's hydrophobic cavities.

For comparison, we also captured an AFM image of PPA-Val upon evaporation of its water/methanol solution. As illustrated in Figure 3A, helically twisted aggregates have been formed by the polymer with right-handed rotation (indicated with the arrows). Close examination of the high-resolution image of the aggregates (Figure 3B) indicates that the helically twisted aggregates consist of multiple nano-knots with a uniform diameter of ~ 57 nm. The knots are compactly associated in a twisting way, instead of in an even deposition; the aggregate thus demonstrates a trend of right-handed rotation. The knots are reminiscent of the pearl-necklace formed by PPA-Val upon natural evaporation of its methanol solution.¹⁰ Similar to the formation of pearls, the knots are also driven by a dominant solvophobic effect and further associated together by forming hydrogen bonding via the hydrophilic groups, which are arranged on the outer part of the knots, to minimize the exposure to polar solvent. The association of the hydrophobic residues will construct multiple hydrophobic microenvironments in the polar solvent, which can favor the intercalation of fluorescence probes and inhibit electron transfer to water or methanol molecules. As mica is a typically hydrophilic surface employed in AFM measurement, to exclude the possible influence related with the property of the substrate, we also detect the morphologies of the self-assemblies of PPA-Val on graphite (not shown). It is found that PPA-Val demonstrates similar morphologies of the aggregates of nano-knots when it is deposited on mica and on graphite. It can easily be understood that the noncovalent interaction responsible for the molecular self-assemblies remains almost the same in the fast evaporation process of the solvent. The influence of the solid substrate, which might also exist, however, plays an inferior role in contrast with the strong inter/intra hydrogen bonds and solvophobic effect of the molecules.

Both the fluorescence microscope and AFM reveal complementary images about the self-assembling of PPA-Val in a polar environment. The superhelical aggregates

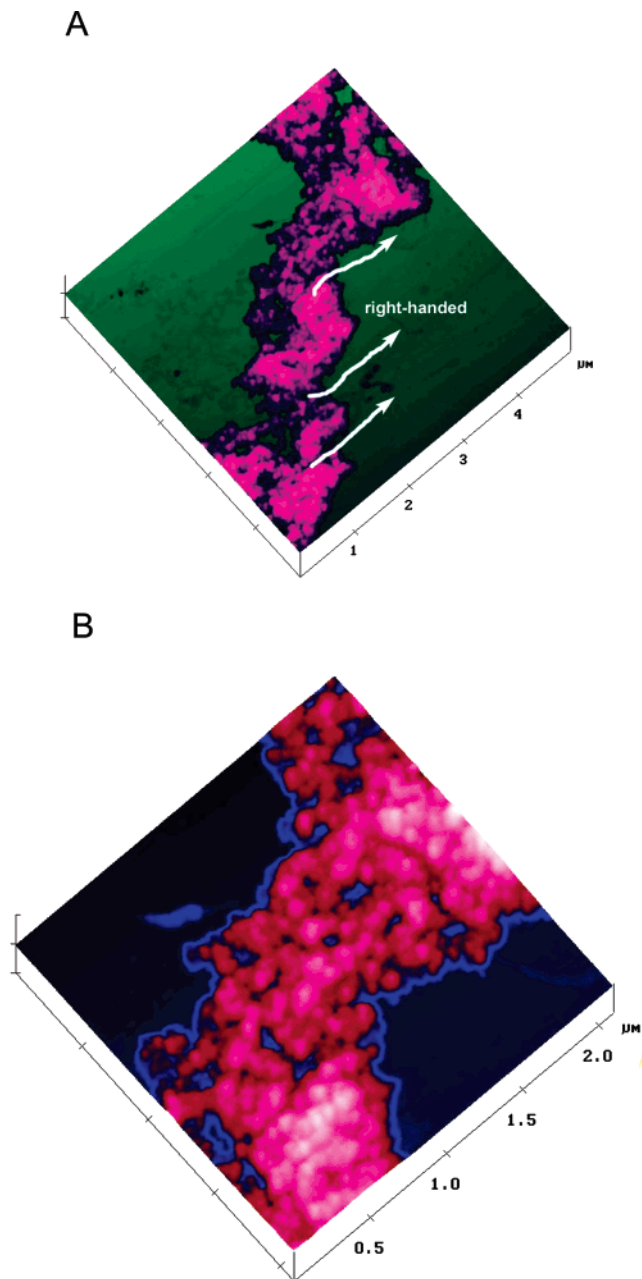


Figure 3. AFM images (A: image in large scale; B: high-resolution image of the nano knots, zoomed in from the middle part of A) of assembled structures formed by PPA-Val from its water/methanol solution ($V_{\text{water}}:V_{\text{methanol}} = 10:1$, concentration of PPA-Val: ~ 0.386 mM) on the surface of mica at room temperature (collected on a Digital Instrument Nanoscope IIIa in tapping mode).

detected with AFM are almost similar to that observed with an in situ fluorescence microscope. Some differences also exist; for example, the former is in a collapsed state due to the evaporation of solvent, while the latter is arranged in a more steric fashion, making the helical tendency easily discerned. On the other hand, AFM is superior to a fluorescence microscope in revealing the details of the nanostructures formed by the polymer. The two methods complete each other in thoroughly revealing the self-assembling of chiral polymer chains in a polar environment. The close-packed aggregates observed with AFM are not formed due to a sharp increase in the polymer concentration in the evaporation process, but are constructed via strong molecular interactions in solution. The results further clarify an intriguing question, that the

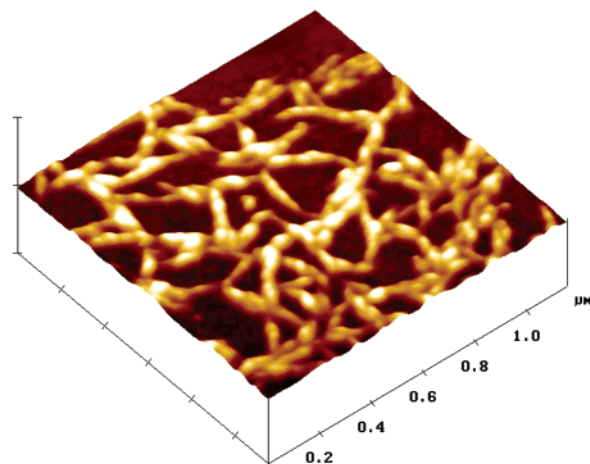


Figure 4. Networks of helical fibers formed by PPA-Val upon natural evaporation of its THF solution with a concentration of $50 \mu\text{g/mL}$.

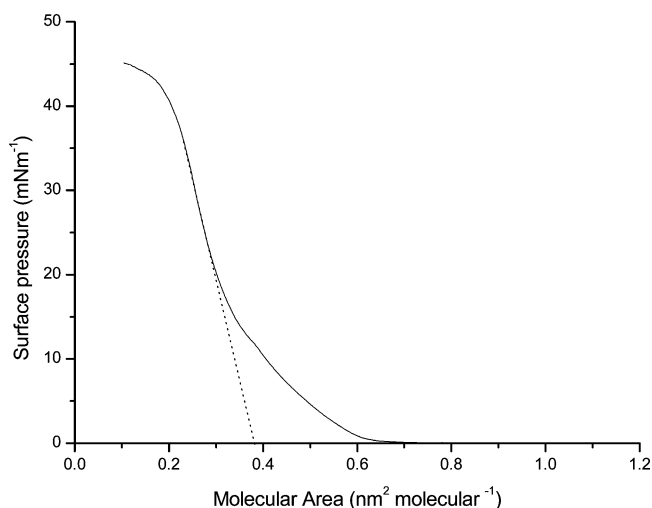


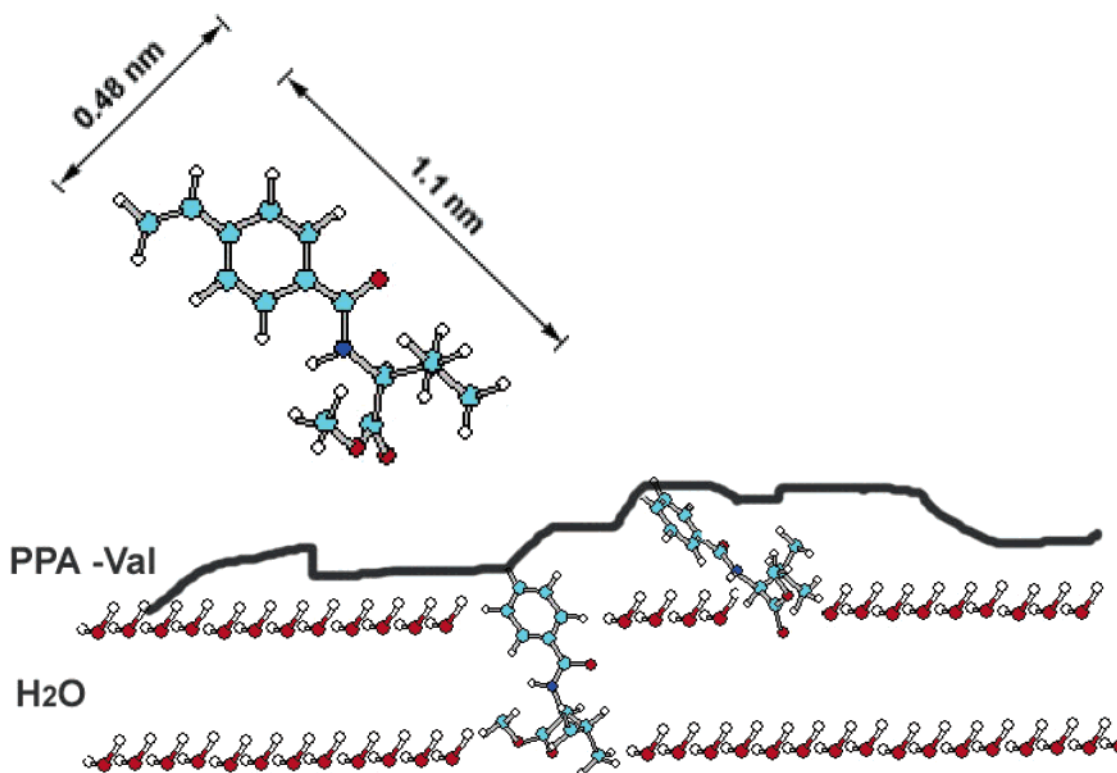
Figure 5. π -A isotherm of PPA-Val on the subphase of water. Concentration of THF solution of PPA-Val: $33 \mu\text{g/mL}$.

helical assembled structures observed with AFM are spontaneously organized in solution prior to deposition. When the polymer solution is deposited on the surface of mica, the substrate or evaporation process causes few changes to the helical structures. Accordingly, AFM can serve as a powerful and feasible tool to investigate the helical assemblies formed in solution. The fluorescence images play an important complementary role to help us understand the helical structures formed by chiral polymers and it will make more sense if they are employed to capture in situ helical reversion. The intercalation of $\text{Ru}(\text{phen})_2(\text{dppx})^{2+}$ to the polymer, on the other hand, also highlights the existence of the hydrophobic internality in the helical assemblies, which are also of great importance in studying the internal properties of the helical assembled structures experimentally. Until now, the existent knowledge about the internality of synthetic helical structure is basically derived from theoretical calculation¹⁵ and experimental evidence is lacking. Our result offers the possibility to characterize the self-assembled helical structures formed by synthetic molecules in solution.

Self-assembling of Helical Polymer on a Water Surface and on a Mica Surface. As discussed above,

(15) (a) Tanatani, A.; Mio, M. J.; Moore, J. S. *J. Am. Chem. Soc.* **2001**, *123*, 1792–1793. (b) Prince, R. B.; Barnes, S. A.; Moore, J. S. *J. Am. Chem. Soc.* **2000**, *122*, 2758–2762.

Scheme 1. Tentative Model for the Adsorbing Behavior of PPA-Val on a Water Surface



the polymer showed similar self-assembled structures when deposited on the surface of mica upon natural evaporation of solution and in solution, because the driving forces under both conditions are basically the same. However, if a helical polymer is deposited on the water surface the driving force will become quite different and diverse morphology may also be expected. To explore the self-assemblies of PPA-Val on the surface of water, we first checked the assemblies of helical polymer upon natural evaporation of its THF solution on the surface of mica for comparison. As can be seen from Figure 4, networks are observed, which are constructed via twisting of superhelical fibers. The superhelical fibers have heights of ~ 6.8 – 14.7 nm and widths of ~ 31 – 51.8 nm. In THF, polymer chains can form strong hydrogen bonds between $-\text{NH}$ and $-\text{C}=\text{O}$,¹⁰ which can stabilize the helical rotation of the polymer chains to give superhelical fibers. When THF evaporated, the superhelical fibers were frozen on the surface of mica.

Since PPA is not soluble in water but its amino acid pendants have enough affinity to water, the polymer is expected to form a stable layer on the water surface. We spread the THF solution of PPA-Val on the surface of water and examined the behavior of the polymer. The π - A isotherm of the polymer is shown in Figure 5. By compressing the water surface, the surface pressure gradually increased and finally reached over 40 mN/m, indicative of the formation of compact polymer monolayer. The isotherm exhibits two regions: one is less than 15 mN/m, where the surface pressure region gradually increased with compression, and the other region is a high surface pressure region, where the surface pressure abruptly increased with compression. The limiting molecular area of PPA-Val obtained by extrapolation of the π - A isotherm to the X axis¹⁶ is ~ 0.38 nm² molecule⁻¹.

To get the details of the monolayer assemblies on water, the LB layer of PPA-Val was deposited on the surface of newly cleaved mica and imaged with AFM in tapping mode. The polymer layer is 1.25 ± 0.12 nm high and the thinnest polymer chains are 14.39 ± 2.57 nm wide. PPA-Val exhibited extended fiberlike morphology and is compactly packed in a layer. No superhelical aggregates were formed, which is in sharp contrast to the helical networks formed upon natural evaporation of the solvent on mica surface. To correlate the information derived from the π - A isotherm and that from AFM, we carried out a simulation of the molecular structure of PPA-Val with the HyperChem 6.0 program. The molecular structure is shown in Scheme 1; the scheme was geometrically optimized with HyperChem 6.0. The length of the pendant is ~ 1.1 nm and the width of the pendant is ~ 0.48 nm. If the pendants lay parallel to the water surface, the contact part is nearly a plane and a maximum contact is made, which corresponds to a limiting area of ~ 0.528 nm². For another special circumstance, when all pendants stand perpendicular to water surface, the contact part is nearly a globule and the minimum limiting area is ~ 0.196 nm². The limiting area deduced from the π - A isotherm is between the values under the above two extreme circumstances, therefore it can be concluded that the polymer chains neither lay on water surface with their pendants fully parallel nor vertical to the surface of water. The pendants must partially contact the surface of water with a proper tilting angle to leave the hydrophilic groups exposed to water and the hydrophobic ones toward air. Based on these data, we provide a tentative model to describe the possible adsorbing behavior of PPA-Val on the surface of water. As illustrated in Scheme 1, the polar groups such as $-\text{C}=\text{O}$, $-\text{CO}$, and $-\text{NH}-$ are partially buried in water, while the nonpolar groups are arranged to avoid contacting the water surface to achieve a stable balance between the hydrophobic and hydrophilic effect

(16) Powers, E. T.; Yang, S. I.; Lieber, C. M.; Kelly, J. W. *Angew. Chem., Int. Ed.* **2002**, *41*, 127–130.

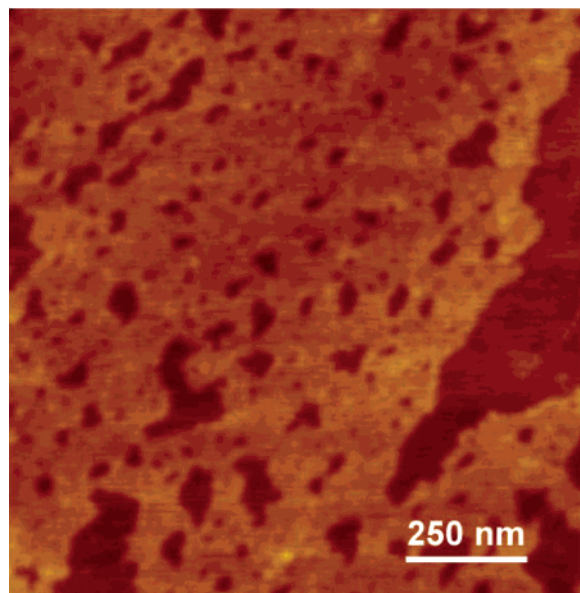


Figure 6. Typical morphology of LB film of PPA-Val transferred to the surface of mica at a surface pressure of 28 mN/m.

of the chiral polymer chains. The polymer chains intertwined with each other randomly and are further compressed into an evenly deposited polymer film.

The influence of water molecules does make a leading role in deciding the arrangement of the chiral polymer chains, as clearly confirmed by a comparison between the self-assemblies formed by the polymer on the surface of mica and on the water surface. On the surface of water, PPA-Val failed to associate into superhelical fibers due to a strong lateral induction of the hydrophobic repulsion between its nonpolar moieties and water molecules. The impacts of water molecules on the self-assemblies of chiral polymer are obviously different in the bulk on and on the surface, which could be easily recognized from the sharp contrast of the polymer's knots-like association in water solution (Figure 3) and the fiber-like assembly on the water surface. The diverse morphological structures are closely related to the different driving forces exerted by water molecules in the bulk solution and on the water surface. It is naturally understood that in water solution polymer chains are surrounded by water molecules and hydro-

phobic repulsions between the polymer chains and water molecules are generated in all directions, which will cooperate to drive the polymer chains to form superhelical aggregates. On the other hand, on the water surface, there is a strong hydrophobic effect concentrated on the lateral area of polymer chains that contact water molecules; superhelical aggregates are thus prevented from association. Instead, the helical twist could only be accomplished within a quite limited number of polymer chains and they are closely packed into the polymer monolayer upon compression.

Self-assemblies of chiral polymers have aroused considerable interest due to their potential application in the field of materials and devices. However, one can only make use of them based on a good understanding of their associations under different conditions. Our study offers an important approach to revealing the different impacts of sample preparation conditions and helps understand the factors involved in molecular assemblies.

Conclusion

We have made a complete investigation of the self-assemblies of chiral polymer chains, in a water/methanol solution, upon the evaporation of solvent on a mica surface and on a water surface. Our results indicate that PPA-Val self-assembled into helical architectures with hydrophobic cavities in a water/methanol solution, and upon natural evaporation of the corresponding solvents the helical aggregates are found to be consisted of nanoknots. However, the assemblies of PPA-Val are quite different on a water surface and on a mica surface upon the evaporation of THF: a monolayer of extended fibers was observed in the former condition and helical fibers were formed in the latter case (see Figure 6), which is attributed to the different strength and manner in which the polymer interacts with water molecules. The diverse self-assembling morphologies of PPA-Val are closely related to the different interactions of polymer and its environmental surroundings.

Acknowledgment. This project is supported by the National Natural Science Foundation of China (No. 20025308, 20177025), the National Key Project on Basic Research (Grant G2000077501), and the Research Grant Council of Hong Kong (HKUST6121/01P).

LA036118L